RSC Advances

ROYAL SOCIETY OF CHEMISTRY

www.rsc.org/advances

Magnesium hydroxide nanoplates/graphene oxide composites as efficient adsorbents for organic dyes

Ju Ran Lee,[a] *Ji Young Bae,*[b] *Wooree Jang,*[a] *Joong-Hee Lee,*[c] *Won San Choi,* *[b] *and Hye Young Koo**[a]

[a]Korea Institute of Science and Technology (KIST) Jeonbuk Institute of Advanced Composite Materials, 92 Chudong-ro, Bongdong-eup, Wanju-gun, Jeollabuk-do, Republic of Korea, E-mail: koohy@kist.re.kr

[b]Department of Chemical and Biological Engineering, Hanbat National University, 125 Dongseodaero, Yuseong-gu, Daejeon 305-719, Republic of Korea, E-mail: choiws@hanbat.ac.kr

[c]Department of Polymer-Nano Science and Technology, Chonbuk National University, Jeonju 561-756, Republic of Korea

Keywords: magnesium hydroxide, graphene oxide, nanocomposites, adsorbents, organic dyes

Abstract

Nanocomposites comprised of magnesium hydroxide ($Mg(OH)_2$) and graphene oxide (GO) were prepared by the controlled precipitation of a magnesium salt on the GO surface. The population of $Mg(OH)_2$ nanocrystals on the GO surface could be varied by varying the $Mg(OH)_2$ precursor amount; the surface area of the resulting $Mg(OH)_2$/GO nanocomposites varied from 75.2 m^2/g to 465 m^2/g. The $Mg(OH)_2$/GO nanocomposite with a surface area of 465 m^2/g showed the best performance. Owing to the synergistic effect of the nanoplate structure of $Mg(OH)_2$ and the 2D structure of GO, the obtained $Mg(OH)_2$/GO nanocomposites exhibited high performance in methylene blue adsorption (adsorption capacity: 779.4 mg/g).

Introduction

The treatment of organic-dye-containing effluents generated by various industries such as textiles, printing, and rubber is a challenging problem in the field of environmental chemistry.[1] Dyes in these effluents can cause damage to living organisms by decreasing the oxygen capacity of water; this disturbs the normal evolution of aquatic life and threatens human health. Because most dye pollutants are hazardous to health and possible cause of cancer, it is essential to develop dye removal materials with high performance and cost efficiency.[2]

Among the various dye removal methods available, adsorption is recommended as an effective method because of its low cost, simple operation, and ability to treat massive amount of dyes.[3-4] Many adsorbents, including activated carbon, silica, clay, polymers, and nanomaterials, have been evaluated to reduce dye concentrations from aqueous solutions.[5-7] As a new group of materials for effective adsorption, graphene—a single layer of sp^2-bonded carbon atoms—has drawn much interest in the field of environmental science because of its high surface area (theoretically, 2640 m^2/g) and 2D structure.[8-11] As a noteworthy derivatives of graphene, graphene oxide (GO) has been used for removing cationic dyes because its negatively charged surface facilitates electrostatic attractions. For example, Yang et al. reported excellent adsorption performance of GO in the removal of methylene blue (MB) from water.[12] It has been demonstrated that the main strength of adsorption is electrostatic interactions, while π–π stacking interactions also contribute to total interactions.[13]

Recently, magnesium hydroxide ($Mg(OH)_2$) has attracted considerable attention because of its wide range of applications such as flame retardant, reinforcing agent, antacid, and

absorbent.[14-18] It is considered as candidate material with price competitiveness for environmental applications because of its ability to effectively adsorb reactive and acid dyes from aqueous solutions. The hexagonal 2D nanostructure of $Mg(OH)_2$ is interesting; however, the adsorption properties of nanostructured $Mg(OH)_2$ have been rarely studied.

In this study, we investigated controllable growth of nanoplate-structured $Mg(OH)_2$ on the surface of GO at room temperature; the resulting $Mg(OH)_2$/GO nanocomposites were evaluated as an effective agent for removing organic dyes from water. The surface area of the nanocomposites could be controlled from 75.2 m^2/g to 465 m^2/g by varying the amount of the magnesium nitride precursor precipitated on the GO surface. Compared with pristine $Mg(OH)_2$, the resulting composites exhibited fast and excellent MB removal capacity, with an adsorption capacity of 779.4 mg/g. This high value was attributed to the favorable attractive interactions between the resulting mesoporous nanocomposites and organic dyes.

2. Experimental

2.1. Materials

Natural graphite powder (>99.8%) was purchased from Alfa Aesar. Sulfuric acid (97%) was purchased from Matsunoen Chemicals Ltd. Potassium permanganate ($KMnO_4$), phosphoric acid (98%), hydrochloric acid (HCl), hydrogen peroxide (H_2O_2), magnesium nitrate hexahydrate ($Mg(NO_3)_2 \cdot 6H_2O$), sodium hydroxide (NaOH), and MB were purchased from Sigma Aldrich and used without further purification. Deionized water with a resistance of 18.2 MΩ cm was prepared from a Millipore Simplicity 185 system.

2.1.1. Synthesis of GO

An aqueous dispersion of GO was synthesized using the modified Hummer's method.[19] In detail, a 9:1 mixture of concentrated H_2SO_4/H_3PO_4 (360 mL sulfuric acid, 98.08%; 40 mL phosphoric acid, 98%) was mixed with 3.0 g of the natural graphite flakes. Subsequently, 18.0 g of 99.3% $KMnO_4$ was slowly added for an overnight reaction. Thereafter, 3 mL of 30 wt% H_2O_2 was added to the resulting suspension, and it was stirred for 1 h. Then, the suspension was subjected to sonication for 30 min at a high level. The resulting suspension was then subjected to centrifugation at 1500 rpm for 30 min and redispersed in 10 wt% HCl to rinse the unreacted residues. This rinsing step was repeated twice, followed by rinsing with DI water twice. To further filter the impurities, the resulting suspension was dialyz ed using DI water. The final concentration of the GO stock solution was controlled to approximately 15 mg/mL and used under dilution if needed.

2.1.2. Synthesis of $Mg(OH)_2$/GO nanocomposites

Ten milliliters of a suspension of graphite oxide (5 mg/mL) in 80 mL of water was ultrasonicated for 2 h to produce a GO suspension. Twenty milliliters of an aqueous solution of magnesium nitrate (0.04 M) was added to this suspension. The mixture was stirred for 5 min at room temperature. To this mixture, an aqueous solution (10 mL) of NaOH (0.5 M) was added dropwise. The mixture was continuously stirred for another 10 min. After reaction completion, a solid was obtained by centrifugation at 8,000 rpm for 5 min; it was washed with methanol four times. After washing, the sample was freeze-dried overnight and a powdered sample was obtained.

2.2. Adsorption of dye from water

Twenty milligrams of the $Mg(OH)_2$/GO nanocomposite was immersed into an MB solution (10 mg/L, 20 mL) while stirring it for a designated time. The MB concentration in the filtrate was measured with a UV-vis spectrophotometer. For recycling of $Mg(OH)_2$/GO, the nanocomposites were washed with ethanol under magnetic stirring for 1 h.

2.3. Material characterization

Field-emission transmission electron microscope (FE-TEM) analyses were carried out using a TECNAI G2 F20 (FEI) microscope. High-angle annular dark-field scanning transmission electron microscopy (HAADF-STEM) was carried out using a JEOL JEM-2200 FS. X-ray diffraction (XRD) patterns were obtained on an X-ray diffractometer (Rigaku, SmartLab) equipped with a Cu Kα source. Absorption spectra were obtained using a UV/vis/NIR spectrophotometer (JASCO, V670). Brunauer–Emmett–Teller (BET) surface areas and Barrett–Joyner–Halenda (BJH) pore-size distributions were measured using an accelerated surface area and porosimetry system (Micromeritics ASAP 2010). Zeta potential measurements were performed on a Malvern Nano ZS Zetasizer at room temperature in water as a solvent.

3. Results and discussion

The $Mg(OH)_2$/GO nanocomposites were synthesized by simple precipitation of a magnesium nitrate precursor on the GO surface, followed by NaOH treatment. We used a dilute magnesium nitrate solution to avoid the rapid generation of $Mg(OH)_2$ nanostructures with poor crystallinity. All the reactions were proceeded at room temperature. The relative amount of the magnesium nitrate precursor was controlled for the synthesis of a series of

$Mg(OH)_2$/GO nanocomposites with a high population of $Mg(OH)_2$ nanoplates with an increased surface area.

The crystallographic structures of the $Mg(OH)_2$ and the $Mg(OH)_2$/GO were identified by XRD. Fig. 1 presents the XRD patterns of $Mg(OH)_2$ and the $Mg(OH)_2$/GO nanocomposites. The diffraction peaks of $Mg(OH)_2$ can be readily identified as the hexagonal brucite phase with lattice constants of a = b = 3.144 Å and c = 4.777 Å (JCPDS card no. 44-1482) and angle constants of $\alpha = \beta = 90°$ and $\gamma = 120°$.[20] In the case of the $Mg(OH)_2$/GO nanocomposites, a shifted (002) peak of GO is observed at around 15° as a shoulder along with the hexagonal-phase peaks of pure $Mg(OH)_2$, indicating successful synthesis of the $Mg(OH)_2$/GO nanocomposites.

To investigate the microstructure of the $Mg(OH)_2$/GO nanocomposites, TEM imaging analyses were performed. TEM analyses of the $Mg(OH)_2$/GO nanocomposites are presented in Fig. 2. Under the experimental conditions used in this study, hexagonal lamellar-shaped $Mg(OH)_2$ and whisker-shaped $Mg(OH)_2$ coexisted, as shown in Fig. 2a. The population of the whisker-structured $Mg(OH)_2$ nanocrystals could be controlled by varying the magnesium nitrate precursor concentration in the reaction. The magnified image of a $Mg(OH)_2$ nanoplate shows a double-layer packed structure, having an empty space between the two layers (Fig. 2b). The $Mg(OH)_2$ nanoplates show a rather narrow size distribution, having an average width and length of 70–100 nm and a thickness of ~10 nm. The selected area electronic diffraction pattern (SAED) of the nanocomposites in Fig. 2c shows well-defined rings, revealing $Mg(OH)_2$ nanoplates on the GO surface with a polycrystalline nature (Fig. 2d). The rings can be indexed to hexagonal magnesium hydroxide,[21] and this agrees with the XRD results. The six diffraction spots with hexagonal patterns result from the presence of GO.

Energy-dispersive X-ray (EDX) elemental mapping studies were also performed to confirm the presence of magnesium in the samples. Figure S1 shows the bright- and dark-field STEM images of prepared $Mg(OH)_2$ and the corresponding elemental mapping images of Mg and O. Fig. S1c shows magnesium in the $Mg(OH)_2$ region and oxygen dispersed throughout the whole nanocomposites.

The population of $Mg(OH)_2$ on the GO surface and the subsequent surface area of the $Mg(OH)_2$/GO nanocomposites could be controlled by adjusting the concentration of the magnesium nitrate precursor. Figure 3 shows a series of TEM images corresponding to varying magnesium nitrate concentration, with other experimental conditions fixed. As the precursor concentration increases, the amount of $Mg(OH)_2$ synthesized on the GO surface also increases, resulting in increased coverage. With increasing $Mg(OH)_2$ population, the surface area of the resulting nanocomposites also tends to increase. The relative N_2 adsorption–desorption isotherm curve of the $Mg(OH)_2$/GO nanocomposites shown in Fig. 4a reveals that they had a porous structure. The average pore diameter was calculated as 9.9 nm by using a BJH model (Fig. S2), revealing a mesoporous structure of the nanocomposites.[22] The mesoporous structure could result mainly from the presence of the $Mg(OH)_2$, because the pristine $Mg(OH)_2$ was found to have similar mesoporous character (Fig. S3). Theoretically, the surface area of graphene reaches up to 2640 m^2g^{-1} because its 2D characteristics make it possible to maximize exposure to various chemicals.[23] However, in actual synthesis, such a high surface area is hardly achieved owing to incomplete exfoliation and the subsequent low yield of single-layered graphene. In our study, the BET surface area of as-prepared GO was found to be around 75.2 m^2g^{-1}. In the case of the $Mg(OH)_2$/GO nanocomposites, the BET surface area tended to increase as the $Mg(OH)_2$ population on the GO surface increased up to

465 m^2g^{-1} under our experimental conditions by increasing the amount of the 0.04 M magnesium nitrate precursor up to 100 mL. Because of their structure, the nanoplates preferred to nucleate and grow along the GO plane axis during the early growth stage.[24] As the amount of magnesium nitrate increased, the nanoplate length increased further and some nanoplates started to point out from the GO basal plane. Owing to this growth aspect, the surface area of the resulting $Mg(OH)_2$/GO nanocomposites could be increased by increasing the amount of the magnesium nitrate precursor. It is worth noting here that the size distribution of the $Mg(OH)_2$ nanoplates was quite monodisperse under our experimental conditions, which included a dilute solution of magnesium nitrate and NaOH. It is known that the use of a dilute solution of the magnesium nitrate precursor results in slow growth of $Mg(OH)_2$ and new nucleation is inhibited, resulting in monodisperse $Mg(OH)_2$ nanocrystals.[25] But, clearly there is a saturation point on increase of surface area because if the amount of the $Mg(OH)_2$ exceed to some limit on the surface of the GOs, aggregation or irregular growth of the $Mg(OH)_2$ appears and the composites also starts to aggregate each other, lowering its specific surface area. When the amount of the magnesium nitrate precursor exceeds 100 mL, this kind of phenomena could be observed in our experiment.

We believe that the $Mg(OH)_2$/GO nanocomposites prepared in this study can be used for various applications owing to their increased surface area and abundance of functional groups on their surface. We tested the resulting nanocomposites for removing organic dyes from water. MB is one of the most commonly used dyes in various industries and was thus selected as a model dye. For all experiments, the initial concentration of the MB solution was kept constant at 10 mg/L; the initial volume was 20 mL. For best performance, the $Mg(OH)_2$/GO composite prepared by using 100 mL of magnesium nitrate precursor (surface area of 465

m^2g^{-1}) is used as an adsorbent for the MB. Figure 5 presents the temporal evolution of UV-vis spectra for the MB solution. Prior to treatment with the $Mg(OH)_2$/GO nanocomposites, MB absorbance was intense; however, right after treatment with the nanocomposites, it decreased dramatically. About 97% of MB was adsorbed within 1 min, indicating the rapid adsorption performance of the $Mg(OH)_2$/GO nanocomposites. Further, the maximum adsorption capacity of the nanocomposites was determined to be 779.4 mg g^{-1}; this value was calculated on the basis of the absorbance ratio at 664 nm and the molar absorption coefficient of MB and using them in Beer-Lambert's Law.[26] The adsorption capacity of the $Mg(OH)_2$/GO composites were tested for several samples prepared from varying the amount of the magnesium nitrate precursor, and the $Mg(OH)_2$/GO composites of higher surface area showed higher adsorption capacity (Fig. S4). Moreover, the $Mg(OH)_2$/GO nanocomposites could be recycled by washing them with ethanol under simple stirring. Figure 6 shows the adsorption rate of MB after various cycles, revealing its ability to remove MB without any performance degradation. The adsorption efficiency of 99.93% can be reached within 2 minutes in spite of repetitive use. The adsorption efficiency is slowly decreased and we found an average MB removal rate of 86% within 1 min after 12 cycles.

The prior interaction between the $Mg(OH)_2$/GO nanocomposites and MB dye would have been electrostatic attraction because the net charge of the nanocomposites was found to be negative at -51.3 mV. In addition, π–π stacking interactions contribute to adsorption, as previously reported.[12] Because GO itself is an excellent MB remover, we also carried out a control experiment by using as-prepared GOs without $Mg(OH)_2$ nanoplates to adsorb MB. We found that GO was well dispersed in the MB solution and we could not separate GO from the dye solution. Thus, we had difficulty in measuring the UV-vis spectra of the MB solution

after the dye was adsorbed on GO. The hybridization of $Mg(OH)_2$ on GO enabled us to collect the adsorbed dye easily owing to the increased specific gravity of the samples. As a comparative experiment, the pristine $Mg(OH)_2$ adsorbent also prepared and tested for their ability to adsorb the MBs, and the adsorption capacity of the $Mg(OH)_2$ is calculated as 4.19 mg/g (Fig. S5). Actually, the intrinsic property of the $Mg(OH)_2$ itself is found to have little effect on the adsorption of MB as revealed on its adsorption capacity of 4.19 mg/g on adsorption of MB in our work. Because $Mg(OH)_2$ have a slightly cationic character upon our experimental conditions of pH 5, and in this case it wouldn't have any favorable interaction with MB dye. For all this, when it is composited with GO the adsorption capacity of the MB remarkably increased by our experiments. We believe that the main reason for the enhanced adsorption capacity is due to the increase of the surface area of the composites from the nanoplate-structured $Mg(OH)_2$, along with the mesoporous character of the $Mg(OH)_2$ composited on the surface of the GOs. Because when we tested adsorption capacity of the $Mg(OH)_2$/GO composites of lower surface area by reducing the amount of the magnesium nitrate precursor, the adsorption capacity shows poorer behavior (Fig. S4). Even though the Mg(OH)2 itself doesn't play a major role in the adsorption of the MB, the effect of composition leading higher surface area seems to be significant on the adsorption capacity of the MB. Thus, we conclude that the composition of the $Mg(OH)_2$ and the GOs derive synergetic effect on removal of the MBs.

In conclusion, we demonstrated controlled synthesis of $Mg(OH)_2$ nanoplates on the GO surface at room temperature and their use for the efficient removal of dyes. The surface area of the resulting $Mg(OH)_2$/GO nanocomposites could be controlled by varying the

concentration of the magnesium nitrate precursor precipitated on the GO surface. The nanocomposite having a surface area of 465 m^2 g^{-1} showed excellent ability for removing MB from a water solution, with an adsorption capacity of 779.4 mg/g. The synthesized $Mg(OH)_2$ nanoplates on the GO surface are believed to impart a mesoporous structure to the resulting nanocomposites, enabling efficient dye adsorption. Moreover, the presence of $Mg(OH)_2$ on the GO surface helped in preventing the restacking of GO nanosheets and enabled easy collection of dye-adsorbed samples from water. We believe our approach could provide an opportunity for tailoring the surface area and the resultant adsorption property of GO via simple growth of $Mg(OH)_2$ nanoplates. We believe this research presents an exploration of the novel properties of GOs produced by hybridization with inorganic nanomaterials with controllable surface morphology and tunable properties, which could be used for numerous applications.

Acknowledgement

We would like to acknowledge the financial support from the Korea Institute of Science and Technology (KIST) institutional program, the R&D Convergence Program of the Ministry of Science, ICT and Future Planning (MSIP) of the Republic of Korea (Grant CAP-13-2-ETRI, 2014003515), and the Basic Science Research Program of the National Research Foundation (NRF) of the Republic of Korea.

Figure captions

Figure 1. XRD data for (a) pristine $Mg(OH)_2$, (b) synthesized $Mg(OH)_2$/GO nanocomposites.

Figure 2. TEM images of (a) $Mg(OH)_2$/GO showing coexistence of hexagonal lamellar-shaped $Mg(OH)_2$ and whisker-shaped $Mg(OH)_2$, (b) magnified image of a $Mg(OH)_2$ nanoplate, (c) typical image of the $Mg(OH)_2$/GO nanocomposite, (d) selected area electron diffraction (SAED) pattern obtained from image (c).

Figure 3. TEM images of $Mg(OH)_2$/GO nanocomposites synthesized using different amounts of a magnesium nitrate solution (0.04 M): (a) 20 mL, (b) 40 mL, (c) 50 mL, and (d) 100 mL.

Figure 4. (a) N_2 adsorption–desorption isotherm curve for $Mg(OH)_2$/GO nanocomposites, (b) variations in the BET surface area upon variations in the magnesium nitrite precursor concentration.

Figure 5. UV-vis absorption spectra for MB solution before and after treatment with $Mg(OH)_2$/GO nanocomposites.

Figure 6. Adsorption rate of MB on $Mg(OH)_2$/GO nanocomposites upon recycling.

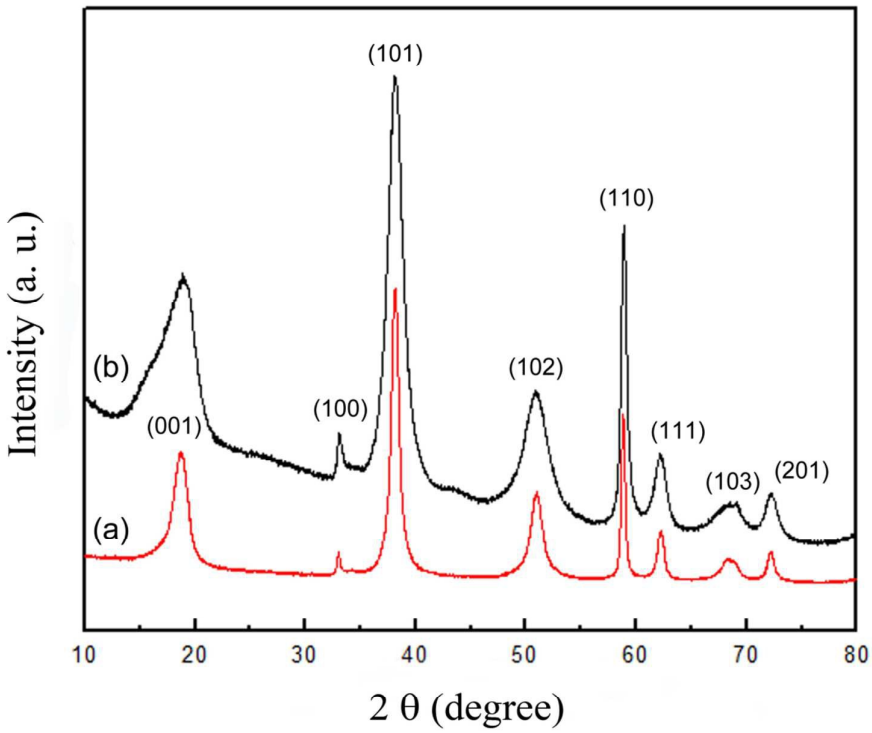

Figure 1

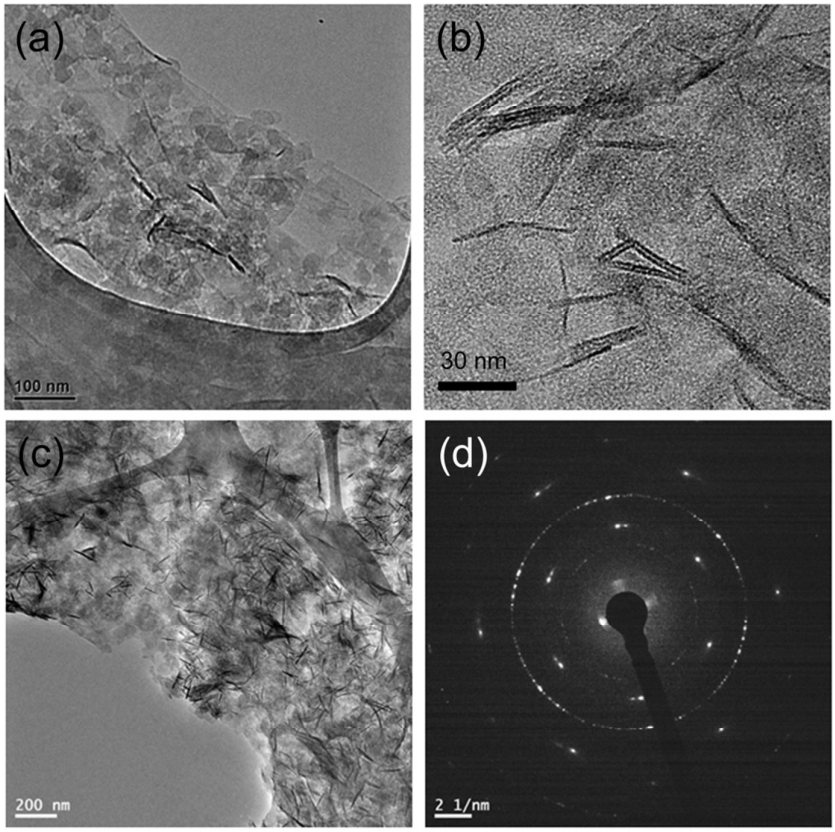

Figure 2

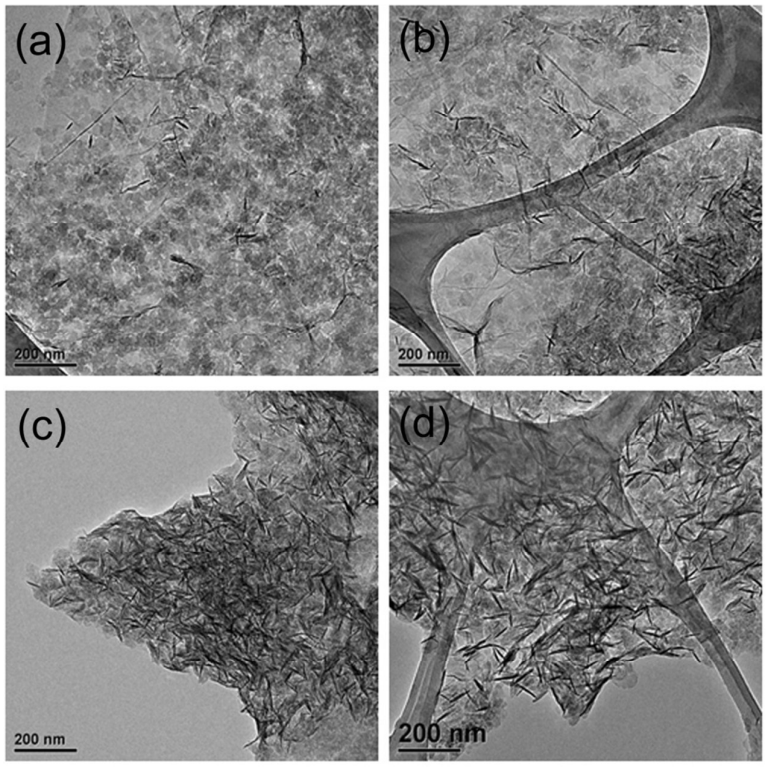

Figure 3

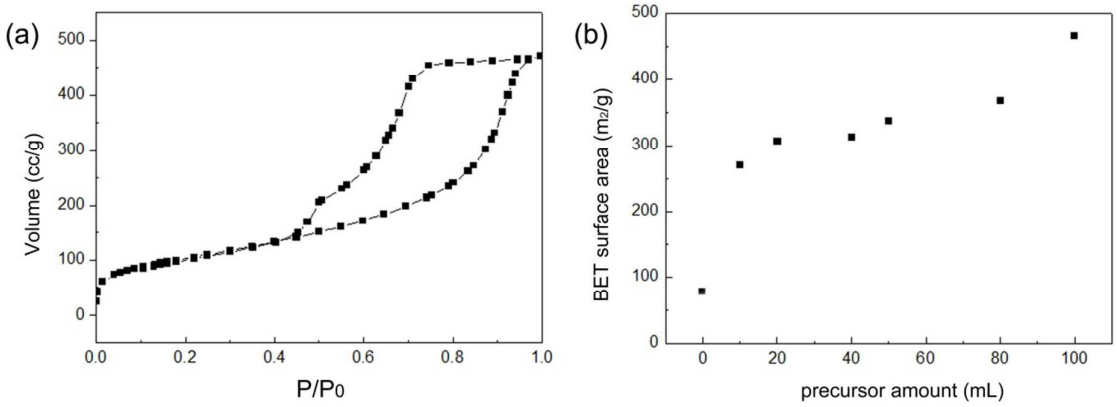

Figure 4

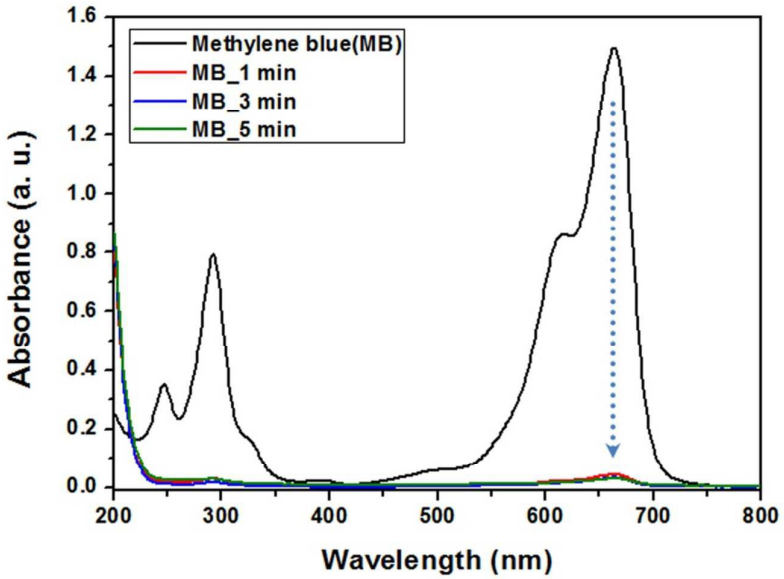

Figure 5

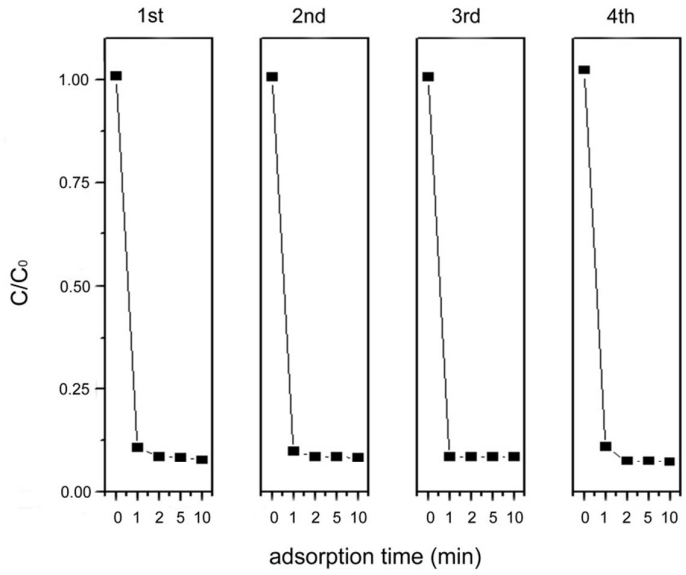

Figure 6

References

[1] M. S. Chiou, P. Y. Ho and H. Y. Li, *Dyes Pigm.,* 2004, **60**, 69-84.

[2] B. Meunier, *Science,* 2002, **296**, 270-271.

[3] N. Kannan and M. M. Sundaram, *Dyes Pigm.,* 2001, **51**, 25-40.

[4] V. Meshko, L. Markovska, M. Mincheva and A. E. Rodrigues, *Water Res.,* 2001, **35**, 3357-3366.

[5] Z. Liu, A. Zhou, G. Wang and X. Zhao, *Chin. J. Chem. Eng.,* 2009, **17**, 942-948.

[6] Y. Ozdemir, M. Dogan and M. Alkan, *Microporous Mesoporous Mater.,* 2006, **96**, 419-427.

[7] S. Lan, L. Liu, R. Li, Z. Leng and S. Gan, *Ind. Eng. Chem. Res.,* 2014, **53**, 3131-3139.

[8] A. K. Geim, *Science,* 2009, **324**, 1530-1534.

[9] Y. Zhang, J. W. Tan. H. L. Stormer and P. Kim, *Nature,* 2005, **438**, 201-204.

[10] X. Wang, L. Zhi and K. Mullen, *Nano Lett.,* 2008, **8**, 323-327.

[11] S. Wang, H. Sun, H. M. Ang and M. Tade, *Chem. Eng. J.,* 2013, **226**, 336-347.

[12] S. T. Yan, S. Chen, Y. Chang, A. Cao, Y. Liu and H. Wang, *J. Colloid Inter. Sci.,* 2011, **359**, 24-29.

[13] B. Li, H. Cao and G. Yin, *J. Mater. Chem.,* 2011, **21**, 13765-13768.

[14] J. Liang and Y. Zhang, *Polym. Int.,* 2010, **59**, 539-542.

[15] W. Z. Liu, F. Huang, Y. J. Wang, T. Zou, J. S. Zheng and Z. Lin, *Environ. Sci. Technol.,* 2011, **46**, 576-582.

[16] Y. D. Li, M. Sui, Y. Ding, G. H. Zhang, J. Zhuang and C. Wang, *Adv. Mater.,* 2000, **12**, 818-821.

[17] R. Giorgi, C. Bozzi, L. G. Dei, C. Gabbiani, B. W. Ninham and P. Baglioni, *Langmuir,* 2005, **21**, 8495-8501.

[18] C. X. Dong, D. L. Song, J. Cairney, O. L. Maddan, G. H. He and Y. L. Deng, *Mater. Res. Bull.,* 2011, **46**, 576-582.

[19] D.C. Marcano, D.V. Kosynkin, J. M. Berlin, A. Sinitskii, Z. Sun and A. Slesarev, *ACS Nano,* 2010, **4**, 4806–4814.

[20] Q. Wang, C. Li, M. Guo, S. Luo and C. Hu, *Inorg. Chem. Front.,* 2015, **2**, 47-54.

[21] J. Chang, H. Xu, J. Sun and L. Gao, *J. Mater. Chem.* 2012, **22**, 11146-11150.

[22] S, Huh, J. W. Wiench, J. C. Yoo, M. Pruski, and V. S. Y. Lin, *Chem. Mater.,* 2003, **15**, 4247-4256.

[23] F. Schedin, A. K. Geim, S. V. Morozov, E. W. Hill, P. Blake, M. I. Katsnelson and K. S. Novoselov, *Nat. Mater.,* 2007, **22**, 652-655.

[24] H. Y. Koo, H. J. Lee, H. A. Go, Y. B. Lee, T. S. Bae, J. K. Kim and W. S. Choi, *Chem. Eur. J.* 2011, **17**, 1214-1219.

[25] Y. Ding, G. Zhang, H. Wu, B. Hai, L. Wang and Y. Qian, *Chem. Mater.,* 2001, **13**, 435-440.

[26] Y. S. Lee, W. Jang, H. Y. Koo and W. S. Choi, *RSC Adv.,* 2015, **5**, 26223-26230.

Table of contents

Magnesium hydroxide nanoplates/graphene oxide composites as efficient adsorbents for organic dyes

Ju Ran Lee,[a] Ji Young Bae,[b] Woori Jang,[a] Joong-Hee Lee,[c] Won San Choi,[b] and Hye Young Koo*[a]*

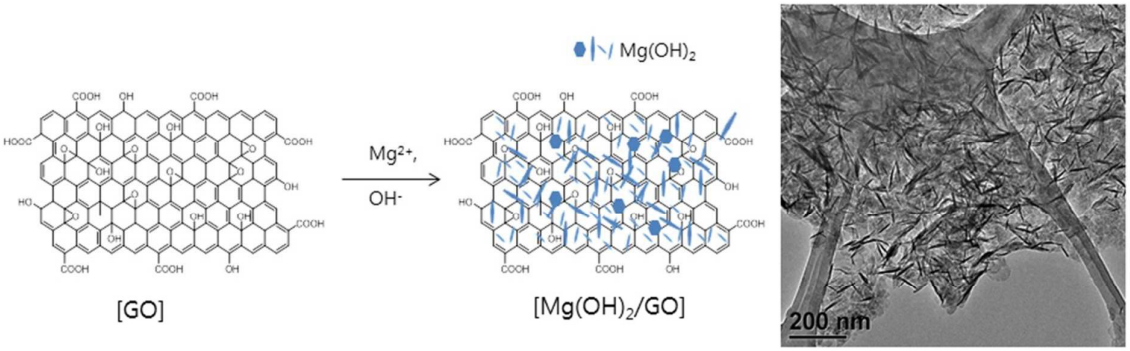

$Mg(OH)_2$ nanoplates/graphene oxide nanocomposites: Controlled synthesis of $Mg(OH)_2$ nanoplates on the GO surface and the use of the resulting nanocomposites for efficient removal of dyes are presented.